Article:

Hu, C., Peng, B., Song, K.X. et al. (2018) The cyan-green luminescent behaviour of nitrided Ba9Y2Si6O24: Eu2+ phosphors for W-LED. Ceramics International, 44 (Suppl 1). S2-S6. ISSN: 0272-8842

https://doi.org/10.1016/j.ceramint.2018.10.166

The Cyan-Green luminescent behaviour of nitrided $Ba_9Y_2Si_6O_{24}$: Eu^{2+} phosphors for W-LED

Congkang Hu,[a] Bing Peng,[a] Kai Xin Song,[a,b]* Bing Liu,[a] Dawei Wang,[b] Ian M Reaney[b]

[a] *College of Electronic Information and Engineering, Hangzhou Dianzi University, Hangzhou 310018, China*

[b] *Department of Materials Sciences and Engineering, The University of Sheffield, Sheffield S1 3JD,U.K*

Available online date provided by the publisher

Abstract

The nitrided $Ba_9Y_2Si_6O_{24}$: Eu^{2+} phosphors were prepared by the conventional high temperature solid state reaction. Si_3N_4 doping obviously improves the luminescent intensity compared with undoped phosphors. The Eu^{2+} emitting lights in different Ba^{2+} crystal lattices and its temperature dependent luminescence properties from 293 to 453K are discussed. Under the 410nm excitation, the nitrided $Ba_9Y_2Si_6O_{24}$: Eu^{2+} has more thermal stability than other same crystal structure of $Ba_9M_2Si_6O_{24}$:Eu^{2+} (M=Sc, Lu, Y). The nitriding schemes can significantly improve the luminescence properties of the phosphors, and nitrided $Ba_9Y_2Si_6O_{24}$: Eu^{2+} can be an excellent candidate as a green phosphor for W-LEDs.

Keywords: $Ba_9Y_2Si_6O_{24}$; Nitride; Phosphors

1. Introduction

The luminescence properties of phosphors directly affect the luminous efficiency, color rendering index (CRI), and color temperature (CT) of W-LED. The color of phosphor can be adjusted to meet the needs of different lighting fields due to the fixed-range emission band of LED chip [1, 2]. At present, partially converting YAG: Ce^{3+} yellow phosphor is a common way to creat a W-LED [3]. But YAG: Ce^{3+} phosphors have defects of low color rendering index and high color temperature, which attributes to the lack of red component in the emission spectrum [4]. Therefore, many researchers have made many attempts to improve the luminescence of YAG phosphors by changing the synthesis method [5]. Setlur et al. [6] studied the luminescent properties of Si_3N_4-doped $RE_3Al_{5-x}O_{12}$: Ce^{3+} (RE=Lu^{3+} or Y^{3+}) phosphors, effectively improved the decay life and thermal stability and realized red-shift of spectrum. Similarly, Sopicka-Lizer et al. [7] used a substituting technique to replace the Al-O bond with a Si-N bond for forming $Y_{2.94}Ce_{0.06}Al_{5-x}Si_xO_{12-x}N_x$ solid solution, which showed that the emission spectrum had a significant red shift. Therefore, Si_3N_4 doping oxide-matrix phosphors have become an important and effective method to improve phosphors' luminescence.

Moreover, nitride phosphors and oxynitride phosphors have received widespread attention because of their high luminous efficiency and thermal stability [8]. However, the nitride compounds are often to be sintered at above 1700°C. On the other side, rare-earth doped silicate phosphors have been favored due to their wide optical spectrum range, good stability, and low cost and suitable synthesis temperature [9, 10, 11]. However, most silicate phosphors have still some shortcomings compared with YAG: Ce^{3+} phosphors in the aspect of luminous efficiencies and thermal stability. In order to further improve the luminescent properties of silicate phosphors, more and more researchers are beginning to use nitriding technology in the study of silicate phosphors. Furthermore, the novel silicate $Ba_9M_2Si_6O_{24}$ (M=Sc, Y, Lu) phosphor has been reported in recent years. T Nakano et al. has prepared $Ba_9Sc_2Si_6O_{24}$:Eu^{2+} phosphor, in which luminescent properties was analyzed, and the effects of Si_3N_4 on the luminescence properties are discussed [12]. Hyun Cho et al. [13] prepared $Ba_9Y_2Si_6O_{24}$: Eu^{2+} phosphor and analyzed the luminescence properties, shown superior luminescence properties relative to $Ba_9Sc_2Si_6O_{24}$: Eu^{2+}. Liu et al. systematically studied the luminescence properties of $Ba_9M_2Si_6O_{24}$: N (N= earth element, M= Sc, Y, Lu), and proved the application prospect of phosphor in white LEDs [14, 15]. But some unclear luminescent mechanism and shortcoming still exist in the aspect of luminous efficiencies and thermal stability compared to commercial YAG: Ce^{3+}. Thus, for the improvement on luminescent performance, we doped Si_3N_4 to actualizing the nitriding process.

In this paper, we reported the Si_3N_4 doped $Ba_9Y_2Si_6O_{24}$: $0.6Eu^{2+}$ phosphors. The effect of nitriding on Eu^{2+} luminescent behaviors of the phosphor was studied. The luminescence properties and thermal characteristics were investigated to different activating center in crystal structures. The overall luminescent performances of nitrided phosphors are better than that of the pristine, which has more possibility to acting as a potential phosphor for W-LED.

2. Experimental section

---

*Corresponding author.
E-mail address: kxsong@hdu.edu.cn (K.X Song)

The samples of $Ba_9Y_{1.94}Si_6O_{24-3x/2}N_x$: $0.6Eu^{2+}$ (x=0-0.4) were synthesized via conventional solid-state reaction. The raw materials are $BaCO_3$ (SP), SiO_2 (99.99%), Eu_2O_3 (99.99%), Y_2O_3 (99.99%), and Si_3N_4 (99.99%). Every raw material was weighed out according the stoichiometric and thoroughly mixed in the agate mortar by enough grinding. Afterward, the obtained powder was fired at 1400°C in $5\%H_2/95\%N_2$ atmosphere for 4h. Finally, the as-synthesized samples were slowly cooled to room temperature and some white powder was obtained after grinding.

X-ray diffraction (XRD) method (Rigaku, Ultima IV, Japan) with Cu-Ka radiation operated at 40kV and 30mA (k=0.154178nm) were used to confirm the crystal structures of the as-prepared samples. The scanning rate for phase identification was at $8°min^{-1}$, with a 2θ range from 10° to 80°. Spectro-fluorometer system (Fluorlog-3, HORIBA JOBIN YVON, France) equipped with a 450 W Xe-lamp was used to measure the photoluminescence (PL) and photoluminescence excitation (PLE) spectra. The Phosphor-excitation-spectrum and thermal-quenching-analysis system (EX-1000) was used to measure the thermal stability-PL.

3. Results and Discussions

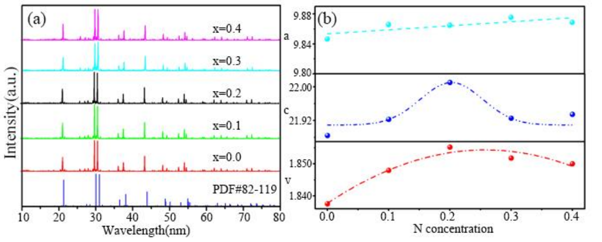

Fig. 1. (a) XRD patterns in $Ba_9Y_2Si_6O_{24-1.5x}N_x$: Eu^{2+} phosphors (x=0, 0.1, 0.2, 0.3 and 0.4); (b) The lattice parameters as a function of x.

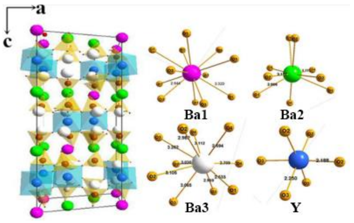

Fig. 2. Structure sketch of $Ba_9Y_2Si_6O_{24}$ host lattice and coordinate environments of Ba1, Ba2, Ba3 and Y with oxygen atoms.

Fig. 1(a) shows all XRD profiles of $Ba_9Y_2Si_6O_{24-1.5x}N_x$: Eu^{2+} (x=0, 0.1, 0.2, 0.3 and 0.4) phosphors were indexed by $Ba_9Sc_2Si_6O_{24}$ (PDF#82-1119) apart from a little amount of Ba_2SiO_4 phase. The XRD pattern is shifted to small angle compared to PDF when x=0, because the ionic radius of Y^{3+} ions (R_Y=0.9Å) is greater than that of Sc^{3+} ions (R_{Sc}=0.745Å). The results indicate that the Eu^{2+} and N^{3-} can completely accommodate in the $Ba_9Y_2Si_6O_{24}$ crystal lattices. The lattice parameters were calculated using the XRD data in Fig. 1(b), which was used to figure out the mechanism for the replacement of a smaller O^{2-} by a larger N^{3-}. It shows that the lattices initially increase with the increase of x, and then begin to shrink when x>0.2. The expansion of lattice is mainly dominated by substitution of bigger ionic radius of N^{3-} ions for smaller ionic radius of O^{2-} ions, and the shrinkage of cell volumes is mainly attributed to oxygen vacancies which will reduce the distance between the activators [16].

Fig. 2 exhibits the layered structure of $Ba_9Y_2Si_6O_{24}$ along with b axis. There are three independent sites, which named Ba(1), Ba(2), and Ba(3) coordinated with 12, 9, and 10 oxygen atoms. Y has only one site coordinated with 6 oxygen atoms. According to previous studies [17, 18], the average bond length of Ba2-O and Ba3-O is very close, and their bond lengths are shorter than that of Ba1-O. Because of the requirement of charge balance and ionic radius, herein, we consider there are two types of luminescent centers when Eu^{2+} ions are doped into the host lattice and occupy Ba^{2+}-sites.

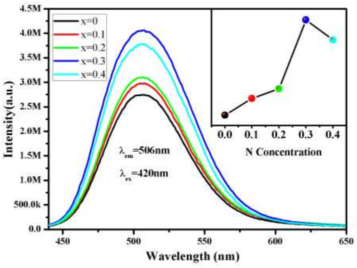

Fig. 3. (a) PL spectra of the $Ba_9Y_2Si_6O_{24-1.5x}N_x$: Eu^{2+} (x=0, 0.1, 0.2, 0.3 and 0.4)

Fig. 3(a) shows the PL spectra of $Ba_9Y_2Si_6O_{24-1.5x}N_x$: Eu^{2+} (x=0~0.4) phosphor under 420nm excitation, which shows a single strong broadband emission centered at 506nm in the 450-600nm band, which can be attributed to the transitions from the 5d excited state to 4f ground states in Eu^{2+} ions. With the increase of N^{3-}, the green emission intensity of $Ba_9Y_2Si_6O_{24-1.5x}N_x$: Eu^{2+} phosphor increases until x=0.3. A further increase in the N^{3-} content in the phosphors led to a clearly concentration quenching of the intensity of Eu^{2+} emission (peaked at 506nm). This phenomenon is ascribed to the energy transfer between the activators. The emission intensity of the phosphor is enhanced because of the N^{3-} replacement O^{2-} in the host, which reducing the distance between the activators is beneficial to the energy transfer between the activators. With N^{3-} concentration increasing, the distance of activators is gradually decreased. When the distance is lower than the critical value, the energy dissipates during the vibration of lattice matrixes, which causes the occurrence of concentration quenching.

Fig. 4(a) shows the PLE spectra of $Ba_9Y_2Si_6O_{24-1.5x}N_x$: Eu^{2+} (x=0-0.4). The excitation curves consist of two shoulder peaks, located at 377nm and 420nm, respectively, which is due to the $4f^7 \rightarrow 4f^65d^1$ transition of Eu^{2+} ion. These phenomena indicate that more than one luminescence center exists in host. To clarify the luminescence centers，Fig. 4(b) shows the PLE spectra and the PL spectra under 377 nm and 420 nm excitation, respectively. It can be seen that the PL spectra edge overlaps substantially, but the emission band is not symmetrical. According to the crystal structure of $Ba_9Y_2Si_6O_{24}$, the average bond of the 9-fold Ba(2) site

(2.925(4) Å) is similar to that of the 10-fold Ba(3) site (2.934(1) Å), leading to a similar crystal-field strength between Ba(2) and Ba(3). while the average bond of the 12-fold Ba(1) site (3.085(3) Å) is longer than that of Ba(2) and Ba(3).

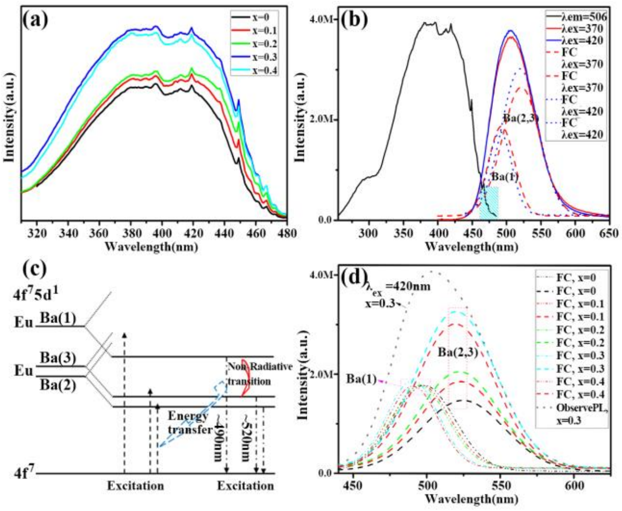

Fig. 4. (a) PLE spectra and (b) PLE and PL spectra of $Ba_9Y_2Si_6O_{23.55}N_{0.3}$: Eu^{2+}; (c) Schematic energy diagram of excitation and emission of Eu^{2+} in different crystallographic sites; (d) the PL spectra of Ba(1) sites and Ba(2, 3) sites; (FC means Fitting curve)

So, the emission band can be deconvoluted only as two bands peaking at ~490 and ~520 nm in Fig. 4(b). The bond lengths sort is Ba(1)−O > Ba(3)−O > Ba(2)−O, indicating crystal-field strength of Ba(1) is weaker than that of Ba(2) and Ba(3). So, Therefore, the cyan lights peaking at 490 nm with higher energy emission band should arise from Eu^{2+} at the Ba(1) site, and Eu^{2+} at the Ba(2) and Ba(3) sites give rise to green lights peaking at 525nm. It is noted that the PL band of Ce-Ba(1) centers overlaps with the PLE band in Fig. 4(b), which infers that it is possible for ET (Energy Transfer) taking place from Eu-Ba(1)-centers to Eu-Ba (2, 3)-centers.

Fig. 4(c) shows the excitation and emission of Eu^{2+} of $Ba_9Y_2Si_6O_{24-1.5x}N_x$: Eu^{2+} in the different crystallography sites, and depicts the energy transfer from Eu-Ba(1)-centers to Eu-Ba (2, 3)-centers. As shown Fig. 4(d), when x=0.3, the emission intensities of Eu^{2+} in Ba(2, 3) sites is about 57% as high as that of x=0, and that of in Ba(1) sites basically unchanged. As a result, the nitrification does not affect the energy transfer from Eu-Ba(1)-centers to Eu-Ba(2, 3)-centers, and only has a great effect on the intensity of Ba(2, 3)-centers.

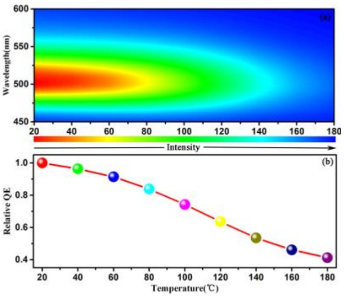

Fig. 5. Temperature dependence of PL spectra (a) and relative external QEs (b) for $Ba_9Y_{1.94}Si_6O_{23.55}N_{0.3}$: Eu^{2+} from 20 to 180 °C.

To understand the underlying relationship between luminescence and temperatures, the PL wavelengths of the 0.03 content of N^{3-} doped $Ba_9Y_2Si_6O_{24-1.5x}N_x$: Eu^{2+} sample in temperatures of 20~180°C have been measured as shown in Fig. 5(a). The emission intensities decrease with increasing temperature until thermal quenching. It should be noted that, as shown in Fig. 5, there are obvious downward trend. When the temperature rises to 180°C, there was a serious thermal quenching. However, the thermal stability of the sample after nitriding was significantly higher than that of the $Ba_9M_2Si_6O_{24}$: Eu^{2+} (M=Sc, Y) phosphor [12, 16]. It is indicated that the addition of N^{3-} can improve the thermal stability of $Ba_9Y_2Si_6O_{24}$: Eu^{2+} phosphors, which is mainly attributed to the stronger covalent rigidity of Si-N bonds than that of Si-O bonds. Fig. 5(b) illustrates the temperature-dependent QE for the optimal $Ba_9Y_{1.94}Si_6O_{23.55}N_{0.3}$: $0.06Eu^{2+}$ samples (The QE values normalized). It drops continuously with temperature increasing due to the thermal quenching effect. About 65% of the initial external QE still can be retained at 120°C. That indicates good thermal stability compared with other many silicate phosphors.

As shown in Fig. 6, with the temperature increasing from 293K to 453K, The emission intensity of the Ba(1)-center and the Ba(2,3)-center are correspondingly weakened. Especially for the Ba(2,3)-center, at 433K, its emission basically disappeared, and the emission of phosphors became mainly emission band of Ba(1)-center. In Fig. 6 (g), the blue line indicates the change of the emission peak position of the phosphor under the 420nm excitation. It can be seen that the peak position gradually shifts to the short-wave direction as the temperature rises, which is attributed to the green luminescence intensity of the Ba(2, 3)-center weakens faster with respect to the Ba(1)-center. The total intensity, Ba(1)-center intensity (~490nm-em) and Ba(2, 3)-center intensity (~525nm-em) with temperature-dependent were shown in Fig. 6(g). It can be seen that the all light bands occur thermal quenching between 293K and 453K, and the green bands peaking at 525 disappears. This phenomenon elucidates that the thermal stability of Eu^{2+} in Ba(1) sites is better stable than that in Ba(2, 3) sites.

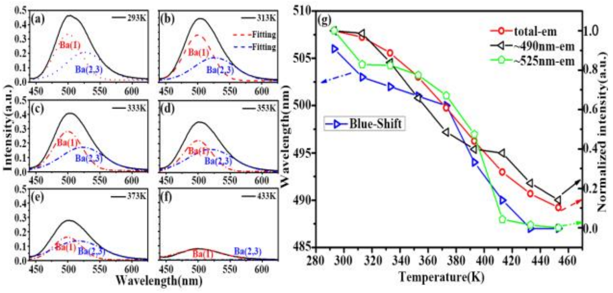

Fig. 6. (a)~(f): The PL spectra about the Gaussian-peaks in different temperature under 420nm exciting(In (a)~(f), the y axis scale is the same); (g) Temperature-dependent luminescence intensities of the three different emission bands (490, 506, and 525 nm) of under 410 nm excitation and Temperature-dependent blue shift.

4. Conclusions

$Ba_9Y_2Si_6O_{24-3x/2}N_x$: $0.6Eu^{2+}$ phosphors were prepared by high temperature solid-state reaction. N^{3-} is penetrated into $Ba_9Y_2Si_6O_{24}$ crystal lattice in replacement of O^{2-} sites, and Eu^{2+} ions occupy the lattice sites of Ba^{2+} ions. Researches show that Nitriding does not change the original crystal structure. To Eu-Ba(1)-center corresponds to short-wave cyan emission peaking at ~490nm and Eu-Ba(2, 3)-center corresponds to long-wave green emission peaking at ~525nm, there is an effective energy transfer from Eu-Ba(1)-center to Eu-Ba(2, 3)-center. With the increase of the Nitriding concentration, the emission intensities of Eu^{2+} in Ba(2, 3) sites are about 57% as high as that of x=0, and that of in Ba(1) sites basically unchanged. As a result, the nitriding does not affect the energy transfer from Eu-Ba(1)-centers to Eu-Ba(2, 3)-centers, and only has a great effect on the intensity of Ba(2, 3)-centers. The thermal stability after nitriding was significantly higher than that of the $Ba_9M_2Si_6O_{24}$: Eu_{2+} (M=Sc, Y) phosphors. In summary, nitrided $Ba_9Y_{1.94}Si_6O_{24-3x/2}N_x$: $0.6Eu^{2+}$ phosphors exhibits more excellent luminescent effects and thermal stability than many other same crystal structure of $Ba_9Sc_2Si_6O_{24}$: Eu^{2+} and $Ba_9Y_2Si_6O_{24}$: Eu^{2+} phosphors, which demonstrate that nitriding can significantly increase the luminescence properties of the silicate phosphor, and it has a great potential application for white LED as blue-green light-emitting component.

Acknowledgements

This work was supported by the National Natural Science Foundation of China under grant number: 51672063, 51202051, and Science and Technology Program of Zhejiang Province under grant number: 2016C31110. Open projects of Key Laboratory of inorganic functional materials and devices, Shanghai silicate institutes, Chinese academy of sciences under grant number: KLIFMD201708

References

[1] W. B. Im, N. N. Fellows, S. P. Denbaars, R. Seshad. $La_{1-x-0.025}Ce_{0.025}Sr_{2+x}Al_{1-x}Si_xO_5$ solid solutions as tunable yellow phosphors for solid state white lighting. Journal of Materials Chemistry, 2009, 19:1325.

[2] Q. Zhang, J. Wang, M. Zhang, Q. Su. Tunable bluish green to yellowish green $Ca_{2(1-x)}Sr_{2x}Al_2SiO_7$: Eu^{2+} phosphors for potential LED application. Applied Physics B, 2008, 92:195.

[3] S. Nishiura, S. Tanabe, K. Fujioka, et al. Properties of transparent Ce: YAG ceramic phosphors for white LED. Optical Materials, 2011, 33(5): 688-691.

[4] J. S. Kim, P. E. Jeon, J. C. Choi, et al. Warm-white-light emitting diode utilizing a single-phase full-color $Ba_3MgSi_2O_8$: Eu^{2+}, Mn^{2+} phosphor. Applied Physics Letters, 2004, 84(15): 2931-2933.

[5] H. M, H. Fadlalla, C. C. Tang. YAG: Ce^{3+} nano-sized particles prepared by precipitation technique. Materials Chemistry and Physics, 114:99-102.

[6] A.A. Setlur, W.J. Heward, M.E. Hannah and U. Happek. Incorporation of Si^{4+}-N^{3-} into garnet hosts for warm white LED phosphors. Chemistry of Materials, 2008, 20: 6277-6283.

[7] M. Sopicka-Lizer, D. Michalik, J. Plewa, T. Juestel, H. Winkler and T. Pawlik. The effect of Al-O substitution for Si-N on the luminescence properties of YAG: Ce phosphor. Journal of the European Ceramic Society, 2012, 32:1383-1387.

[8] R. J. Xie, N. Hirosaki. Silicon-based oxynitride and nitride phosphors for white LEDs-A review. Science and Technology of Advanced Materials, 2007, 8(7-8): 588-600.

[9] L. E. Muresan, B. F. Oprea, A. I. Cadis, et al. Studies on Y_2SiO_5: Ce phosphors prepared by gel combustion using new fuels. Journal of Alloys and Compounds, 2014, 615: 795-803.

[10] H. K. Yang, H. M. Noh, B. K. Moon, et al. Luminescence investigations of Sr3SiO5: Eu2+ orange–yellow phosphor for UV-based white LED. Ceramics International, 2014, 40(8):12503-12508.

[11] J. K. Han, A. Piqutte, M. E. Hannah, et al. Analysis of $(Ba, Ca, Sr)_3MgSi_2O_8$: Eu^{2+}, Mn^{2+} phosphors for application in solid state lighting. Journal of Luminescence, 2014, 148: 1-5.

[12] T. Nakano, Y. Kawakami, K. Uematsu, T. Ishigaki, K. Toda, and M. Sato, Novel Ba–Sc–Si-oxide and oxynitride phosphors for white LED. J. Lumin. 129, 1654 (2009).

[13] J. H. Ryu, O. G. Jeong, J. C. Park, et al. Synthesis and photoluminescence of novel $Ba_9Y_2Si_6O_{24}$: Eu^{2+} green phosphor. Journal of Nanoscience & Nanotechnology, 2013, 13(9):6086.

[14] K. Song, J. Zhang, Y. Liu, et al. A Red-Emitting Phosphor Ba9Lu2Si6O24: Ce3+, Mn2+ with Enhanced Energy Transfer via Self-Charge Compensation. Journal of Physical Chemistry C, 2015, 45(14):24558-24563.

[15] Y. Liu, J. Zhang, C. Zhang, et al. High Efficiency Green Phosphor $Ba_9Lu_2Si_6O_{24}$: Tb^{3+}: Visible Quantum Cutting via Cross-Relaxation Energy Transfers. Journal of Physical Chemistry C, 2016, 120(4):2362-2370.

[16] Y Liu, Z Xia, Z Hao,l. Generating yellow and red emissions by co-doping Mn^{2+} to substitute for Ca^{2+} and Sc^{3+} sites in $Ca_3Sc_2Si_3O_{12}$: Ce^{3+} green emitting phosphor for white LED applications, Journal of Materials Chemistry, 21 (41) (2011) 16379-16384.

[17] B.Peng, K.X. Song, H.W.Wang, et al. Investigation on Ce^{3+}luminescence from different crystallographic sites, self energy transfer and abnormal thermal stability of nitrided $Ba_9Y_2Si_6O_{24}$: Ce^{3+}phosphor for W-LEDs. Ceramics International, 2018, 44(6):6584-6589.

[18] Liu Y, Zhang C, Cheng Z, et al. Origin and Luminescence of Anomalous Red-Emitting Center in Rhombohedral $Ba_9Lu_2Si_6O_{24}$:Eu^{2+} Blue Phosphor. [J]. Inorganic Chemistry, 2016, 55(17):8628-8635.